

# Dehydrogenation and Other Non-radiative Relaxation Processes in Gas-Phase Metal–DNA Base Complexes

David B. Pedersen,\* Marek Z. Zgierski, and Benoit Simard

Steacie Institute for Molecular Sciences, National Research Council of Canada,  
Ottawa, Ontario, Canada, K1A 0R6

Received: March 28, 2003; In Final Form: May 22, 2003

Photoinduced dehydrogenations of gas-phase Al–guanine, Mn–guanine, and the Al–base pair adduct Al–guanine–cytosine have been observed. Upper and lower limits on the minimum photon energy required to effect the dehydrogenation have been determined for these species. Species were generated using a laser ablation source and were detected with laser photoionization/time-of-flight mass spectrometry. Only metalated species were observed to dehydrogenate, and the effect of metal on the photochemistry of guanine and cytosine has been investigated using density functional theory (DFT). Avoided crossings between the ground and first electronically excited states are features specific to the metalated species and are likely responsible for the metal-specific dehydrogenation observed. The rapid nonradiative relaxation believed to manifest the dehydrogenation is consistent with the dominance of multiphoton contributions to the mass spectral signals observed which also stems from rapid nonradiative relaxation. In this context, the photophysics of the gas-phase complexes is similar to that of solution-phase bases where nonradiative relaxation processes also dominate.

## 1. Introduction

Recent gas-phase studies of an Al–cytosine complex<sup>1</sup> have shown that metal–DNA base interactions manifest novel dissociation pathways and added complexity to the already complex, dominantly nonradiative, relaxation mechanisms of photoexcited DNA bases. As fundamental photochemical processes, the nonradiative relaxation mechanisms of the DNA bases are remarkably efficient and the near-immunity of the bases to UV-induced damage is attributable to this characteristic. The effect of metal interactions on DNA base photochemistry and relaxation mechanisms is relatively unexplored, but it impacts on biochemistry where UV damage and metal-induced DNA mispair formation processes<sup>2</sup> are topics of interest. The relatively novel field of DNA-based nanomaterials where, for example, self-assembly of DNA–metal nanoparticle arrays has been demonstrated,<sup>3,4</sup> also sparks interest in the effect of metals on DNA photochemical and photophysical processes.

The prevalence of nonradiative relaxation processes in DNA bases is well established. The fluorescence quantum yield associated with excitation in the UV is extremely small ( $\phi \approx 10^{-4}$ )<sup>5</sup> as is the phosphorescence quantum yield.<sup>6,7</sup> The low overall quantum yield for emission is a clear indication that the absorbed UV is dissipated almost exclusively via internal conversion and/or intersystem crossing mechanisms. Accordingly, the recently measured lifetimes of the  $S_1$  states of adenosine, cytidine, thymidine, and guanosine nucleosides are relatively short, falling within the 290 to 540 ( $\pm 40$ ) fs range.<sup>8,9</sup> These studies have also shown that following excitation with 263 nm laser light, the rate of internal conversion to  $S_0$  is greater than the rate of vibrational energy exchange with the solvent. Thus, energy is conserved during the internal conversion

process, and the  $S_0$  state is initially created with an excessive amount of vibrational energy. The initial vibrational temperature is estimated to be approximately 1200 K. Similarly, the  $S_1$  states of the DNA bases in water solutions are found to have lifetimes of 1 ps.<sup>10</sup>

Study of the DNA bases in the gas phase affords an opportunity to examine photochemistry and photophysics free of the bath effect of solvent. One advantage of the gas-phase medium is that dissociation processes are more readily identifiable. A second is that solvent-promoted curve-crossing is avoided and the efficiencies of internal conversion processes are determined entirely by the nature of the electronic states of the DNA bases. That is, internal conversion can be interpreted free of perturbations and specifically in terms of the crossing of molecular potential energy curves characteristic of the gas-phase species. For example, the rate of population of  $S_0$  of gas-phase guanine appears to be orders of magnitude slower than in solution. A priori, this result is not necessarily expected as internal conversion processes are known to occur relatively efficiently in gas-phase molecules.<sup>11,12</sup> Experiments have shown, however, that the delay between an initial photoexciting laser pulse and a subsequent ionizing laser pulse can be as long as 10  $\mu$ s and ionization of guanine still occurs.<sup>13</sup> This observation suggests that a relatively long-lived electronically excited state of guanine, from which ionization by the second laser occurs, is populated. This long-lived state is thought to be the lowest energy triplet ( $T_0$ ) populated via an intersystem crossing process.

Due to the short (femtosecond) time-scale for relaxation of electronically excited DNA bases, resonant-enhanced photoexcitation processes may exhibit a dependence on laser power characteristic of multiphoton excitation processes. Following Parker et al.<sup>14</sup> the rate equations associated with a two-photon ionization process are

\* Author to whom correspondence should be addressed. E-mail: david.pedersen@nrc-cnrc.gc.ca.



where  $A$  and  $A^*$  are the ground and electronically excited states, respectively,  $A^+$  is the ionized species,  $\sigma$  and  $\sigma'$  are the absorption cross sections for excitation and ionization, respectively,  $h\nu$  denotes absorption of a photon, and  $\gamma$  is the phenomenological rate of nonradiative relaxation of  $A^*$ . From this scheme, the observed ion signal intensity is given by

$$\text{signal} \propto \frac{N_A \sigma \sigma' I^2}{\sigma' I + \gamma} \quad (4)$$

where  $N_A$  is the number density of  $A$ , and  $I$  is the intensity of the laser pulse imposed on  $A$ . From eq 4 it can be seen that when  $\gamma$  is much smaller than  $\sigma' I$ , i.e.,  $A^*$  is relatively long-lived, the observed ion signal will display a first-order dependence on  $I$ . This is the case typically associated with resonantly enhanced multiphoton ionization spectra. When  $\gamma$  is much greater than  $\sigma' I$ , i.e.,  $A^*$  is relatively short-lived, the observed ion signal will display a second-order dependence on  $I$ . In this case, the lifetime of  $A^*$  is somewhat comparable to the lifetime of the virtual state initially populated in a simultaneous two-photon absorption process. Note that in the scheme presented, eqs 1–3, the excitation process is resonant, unlike the simultaneous absorption process involving population of a virtual state, but displays the same power dependence as the simultaneous absorption process. Thus, for resonant processes, a second-order dependence indicates that the lifetime of the intermediate state,  $A^*$ , is short. That is the dependence of signal intensity on laser intensity can be used to characterize, to some extent, the intermediate state lifetime.

Precedent studies of the effects of metal on DNA base photochemistry and photophysics are few. It has been shown that DNA-bound Os(phen)<sub>2</sub>dppz<sup>2+</sup> and Ru(phen)<sub>2</sub>dppz<sup>2+</sup> yield similar charge-transfer rates and efficiencies in solution, suggesting that in such ligated compounds the nature of the metal has little effect on photoinitiated charge transport.<sup>15</sup> For bare metal centers, however, other studies suggest that the metal does affect the orbital structure of DNA bases and that this effect is metal-specific. For example, theory shows that the  $d_{z^2}$  orbital of Pt<sup>2+</sup> interacts with the  $\pi$  orbitals of cytosine while for Hg<sup>2+</sup> similar interactions are relatively weak.<sup>2</sup> Theoretical studies of metal ion–nucleic base complexes have also been published.<sup>16,17,18</sup> In previous work we acquired the photoionization efficiency spectrum of an Al–cytosine complex.<sup>1</sup> This molecule was found to display photochemistry very different from that of cytosine. In particular, relatively efficient two-photon dehydrogenation of the complex was observed.

In this paper we have expanded our study of gas-phase metal–DNA base complexes to include Al–guanine, Mn–guanine, and the metal–base pair adduct Al–guanine–cytosine. This survey of metal–DNA base photochemistry was initiated in hopes of establishing some generalities or trends in metal–DNA base photochemistry. We find that dehydrogenation of all of the metal–DNA base complexes occurs and the threshold energies for the onset of dehydrogenation have been measured. Dehydrogenation is found to result from population of an electronic state that is repulsive in the N–H coordinate; the dissociation is not a statistical (RRKM) process. We also present

evidence that electronically excited states of metal–DNA base complexes can be short-lived, the lifetime being shortened by relatively efficient nonradiative relaxation processes. In this context, the photophysics of the gas-phase metal–DNA base complexes resembles that of the solution-phase DNA bases.

## 2. Experimental Section

The laser ablation/photoionization mass detection apparatus has been described previously.<sup>19</sup> The only significant difference in the present experiments was the use of pressed powder metal–DNA base rods. Combinations of Al (Fisher Scientific, 20 mesh and finer) or Mn (Johnson-Matthey, 325 mesh, 99.3%) powders with guanine (Aldrich, 97% pure) or cytosine (Aldrich, 97% pure) powders were mixed together, in an approximately 30%:70% volume ratio, using a mortar and pestle. For Al–guanine–cytosine the ratio was approximate 30%:35%:35%. These mixtures were then placed into a 6 mm diameter cylinder into which a 6 mm piston was forced by applying a pressure of 2500 psi ( $1.7 \times 10^7$  Pa). Pressure was maintained for approximately two minutes, after which the pressed rod was removed and placed in the ablation chamber of the apparatus. The apparatus consists of source and detection chambers. The source chamber contains a Smalley-type laser ablation source where the pressed powder rod is ablated in the throat of a pulsed valve. The rod was ablated with approximately  $500 \mu\text{J pulse}^{-1}$  355 nm laser (Lumonics YM200) light, focused to a 1 mm<sup>2</sup> spot, synchronous with a He pulse (Jordon piezoelectric valve with 80 psi ( $6 \times 10^5$  Pa) backing pressure) passed over the rod. Species generated by the ablation process are entrained in the He and subsequently expanded through a 1 mm diameter channel into the  $10^{-6}$  Torr ( $10^{-4}$  Pa) vacuum of the first chamber, thus generating a molecular beam. Source conditions were adjusted to maximize the metal–base signal intensity. In the second chamber UV laser light intersected the molecular beam perpendicular to the beam axis. Frequency doubled-tunable dye laser light was used at energies below 6 eV (207 nm) while ArF (6.4 eV) and F<sub>2</sub> (7.9 eV) excimer lasers were used to ionize species at higher energies. Ionization laser fluences were measured using OPHIR/NOVA and Gentec Duo/ED-500 power meters. Species were ionized in the extraction region of a reflectron time-of-flight mass spectrometer equipped with an MCP detector.

## 3. Results

A mass spectrum illustrating the types of species distributions generated by the laser ablation source is shown in Figure 1. This spectrum was collected via ablation of an Al–guanine–cytosine rod and an ionization laser wavelength of 157 nm. As seen, the source produces a distribution of metal-free species along with their metal adducts. As for Al–cytosine,<sup>1</sup> by varying the ionization laser wavelength the onset of dehydrogenation of metal–DNA base adducts was observed. A sample of the type of data collected is shown in Figure 2.

At an ionization laser energy of 5.915 eV (209.6 nm), a single peak corresponding to Al–guanine is observed in the time-of-flight mass spectrum. At 5.928 eV (209.15 nm) a new feature is observed at shorter flight time (lower mass). This peak corresponds to dehydrogenated Al–guanine. Using this technique the threshold for dehydrogenation of Al–cytosine,<sup>1</sup> as well Al–guanine, Mn–guanine, and Al–guanine–cytosine have been determined. These results are collected in Table 1. Upper limits shown in the table correspond to the longest wavelengths at which clear evidence of dehydrogenation was observed. Lower limits correspond to the shortest wavelengths

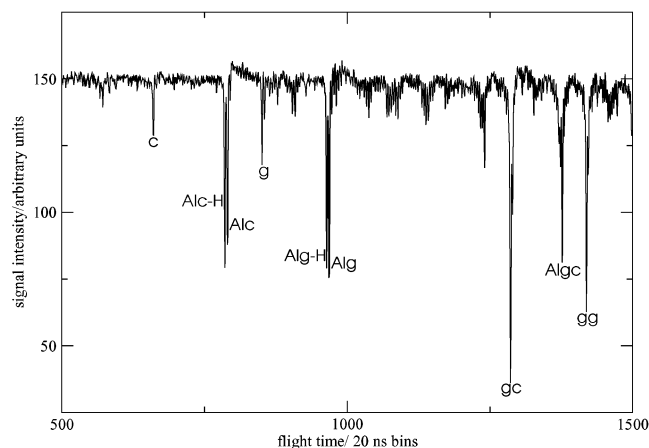


**Figure 1.** Mass spectrum of species generated upon ablation of an Al-cytosine-guanine rod. Species were ionized using 157 nm laser light. g denotes guanine, c denotes cytosine, and -H denotes a dehydrogenated (loss of H) species.

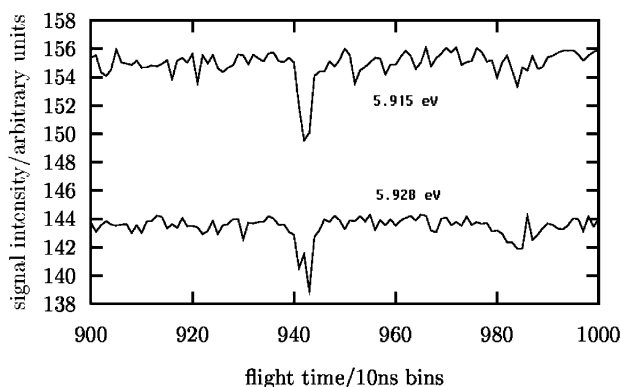


**Figure 2.** Mass spectra of Al-guanine taken at 209.6 nm (5.915 eV) and 209.15 nm (5.928 eV) ionization laser wavelengths. The two spectra are offset vertically for clarity. At 209.15 nm a new feature appears as a shoulder in the spectrum. The peak corresponds to dehydrogenated Al-guanine. This process is thought to involve absorption of two photons (see text for details).

**TABLE 1: Threshold Energies for Dehydrogenation of Metal–DNA Base Complexes (units of eV)<sup>a</sup>**

species	upper limit	lower limit
Mn-guanine	7.90	5.96
Al-guanine	5.928	5.915
Al-cytosine	6.42	5.70
Al-guanine-cytosine	7.90	5.90

<sup>a</sup> Between upper and lower limits laser light of sufficient intensity could not be generated with the lasers available, as described above. The 6.42 eV laser functioned only for the Al-cytosine experiments.

at which no evidence of dehydrogenation was observed. The wavelengths examined are limited by the availability of dyes and/or pump lasers, and the energies between the limits shown in Table 1 correspond to wavelengths that could not be investigated with the laser systems available to us, as described above. For a given metal–base complex, dehydrogenation is observable at many wavelengths above threshold as shown in Figure 3.

The effect of ionization laser fluence on signal intensity is illustrated in Figure 4. As seen, plots of log of the signal intensity vs log of ionization laser power were found to be linear with slopes usually greater than one, as discussed below. Data collected with the ionization laser tuned to 218.55 nm are shown for guanine, Al-cytosine, and Al-guanine.

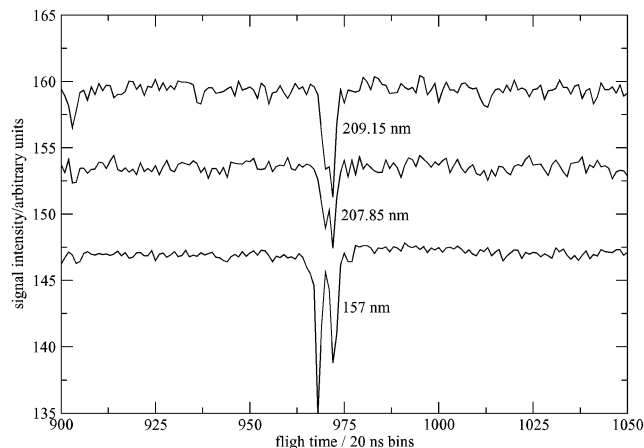


**Figure 3.** Mass spectra of Al-guanine collected by ionizing with the various wavelengths shown. In all spectra, a peak corresponding to Al-guanine and a peak of weaker intensity, usually appearing as a shoulder, corresponding to dehydrogenated Al-guanine are observable. The spectra are offset vertically for clarity.

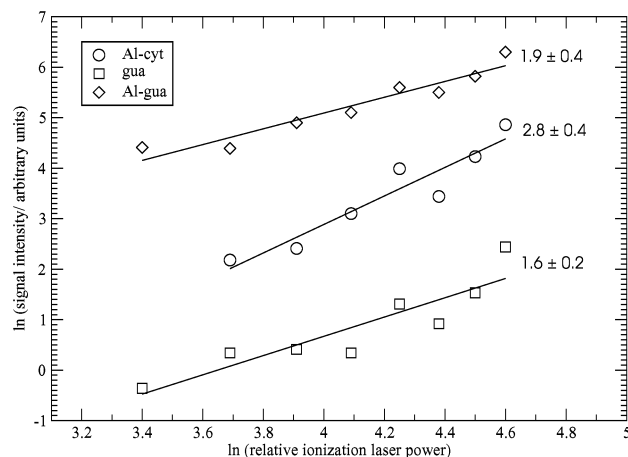


**Figure 4.** Plots of  $\ln(\text{signal intensity})$  vs  $\ln(\text{ionization laser power})$  for guanine, Al-cytosine, and Al-guanine. The ionization laser wavelength was 218.55 nm. The lines are linear regression fits of the data which are shown as points. The slope of the linear regression fit is shown for each species. The data are offset vertically for clarity.

## 4. Discussion

**4.1. The Dehydrogenation Mechanism.** The observation of photoinduced dehydrogenation of Al-cytosine in previous work, and Al-guanine, Mn-guanine, and Al-guanine-cytosine in the present work, is good evidence that dehydrogenation is a general characteristic of metal–DNA base complex photochemistry. Although dehydrogenation of metal–DNA base complexes occurs irrespective of the metal employed, the chemistry involved does require participation of the metal. This is obvious from the observation that within the wavelength ranges examined (220 to 157 nm) only dehydrogenated analogues of metal-containing species are observed in the mass spectra. Furthermore, the energetics of dehydrogenation are found to depend on the nature of the complexed metal. In Table 1 the threshold energies measured for dehydrogenation of the M–DNA base complexes are shown. The values shown are all equivalent, within the experimentally measured limits, except for Mn-guanine. The lower-limit value for dehydrogenation of this complex lies above the upper limit determined for Al-guanine. Dehydrogenation of Mn-guanine is therefore a higher energy process. Thus, although dehydrogenation may occur irrespective

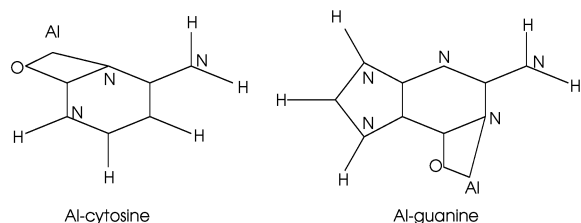


**Figure 5.** Theoretical structures of the ground states of neutral Al-cytosine and Al-guanine.<sup>1,20</sup> Unlabeled atoms are carbon.

of the nature of the metal, the energetics of the process are observed to vary for different metals.

The probability that the observed dehydrogenation results from a statistical (RRKM) dissociation process is low. For a statistical process, where surmounting an energy barrier is rate-limiting, signal associated with the dehydrogenation can be expected to increase gradually as the excitation energy is increased. That is, the increase in signal intensity reflects the increasing probability of surmounting the barrier as a smooth function of the photon energy. Such a smooth increase in probability is not observed for Al-guanine, however, as seen in Figure 2 and Table 1 where the threshold energy for dehydrogenation has been determined very precisely. The ability to define the threshold so precisely implicates a nonstatistical dehydrogenation process likely involving population of a specific electronic state.

The unlikelihood of statistical dissociation contributing to the dehydrogenation observed can also be established using RRK theory. From RRK, the rate of dissociation,  $k$ , for a statistical process is given by

$$k = \nu \left( \frac{E - E_0}{E} \right)^{s-1} \quad (5)$$

where  $E$  is the excitation energy,  $E_0$  is the energy required to dissociate the molecule,  $\nu$  is the vibrational frequency of the critical mode, and  $s$  is the number of active oscillators. To first order,  $s$  is given by  $3n - 6$ , where  $n$  is the number of atoms in the molecule.  $E_0$  is around 2 eV, as predicted by DFT the results of which are shown for Al-cytosine in Figure 6, are shown for Al-guanine in Figure 8, and are discussed below.  $E$  is the threshold energy at which dehydrogenation is observed. These

energetics are illustrated in the Jablonski-type diagram shown in Figure 7. For Al-guanine-cytosine the limiting value for  $E$  is 7.9 eV from Table 1. The frequency of N-H, where dehydrogenation occurs, is  $3400 \text{ cm}^{-1}$ . Substitution of these values into eq 5 yields a value of  $1000 \text{ s}^{-1}$ . That is, the dehydrogenation occurs on the millisecond time scale. This time scale is long in comparison to the time-of-flight mass separation process used in the spectrometer. Accordingly, any dehydrogenated species created via RRK processes will arrive at the detector very late relative to ions formed promptly in the extraction region of the spectrometer. However, this is not the case for the dehydrogenated species observed as they have arrival times (peak positions in the mass spectra) expected for dehydrogenated species. That is, the dehydrogenated species observed in the mass spectrum cannot be formed via the relatively slow statistical (RRK) dissociation process.

To investigate the possibility of photoinduced population of specific electronic states as a dehydrogenation mechanism, TD DFT (B3LYP/6-31++G\*\*) calculations of the electronic states of cytosine and Al-cytosine were performed. The geometries of the complexes are shown in Figure 5, as have been published elsewhere.<sup>1,20</sup> In Figure 6, potential energy curves of the lowest eight electronic states of cytosine and the lowest eleven for Al-cytosine are shown as a function of N-H separation, where N is the ring-constituent nitrogen. To generate these plots, the geometries of the molecules were frozen in their lowest-energy, ground-state configurations except for the N-H bond length which was varied. At each N-H distance the energies of the lowest energy electronic states were calculated, as shown. With this approach, the energetics associated with dehydrogenation cannot be determined quantitatively and a comparison with the measured threshold energies is not possible. It is clear, however, that for dehydrogenation and ionization to occur (as is prerequisite for the observation of dehydrogenated species in the mass spectra) the absorption of two photons is required, as has been discussed in a previous publication.<sup>1</sup> A Jablonski-type diagram illustrating the likely mechanism of formation of the dehydrogenated metal-base species observed is shown in Figure 7.

An initial absorption event, to a state 6 eV above the ground electronic state, is followed by rapid nonradiative relaxation to a dissociative state, compatible with Figure 6 and Figure 8 below. The ensuing dehydrogenation event is followed by

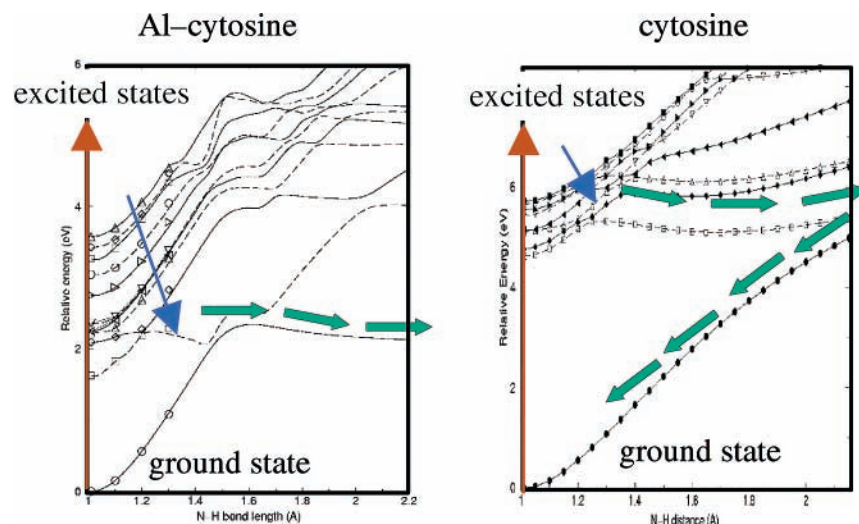


**Figure 6.** Theoretical potential energy curves of the electronic states of cytosine (right) and Al-cytosine (left) as a function of the N-H bond length, where N is the ring-constituent nitrogen. Following an initial photoexcitation, indicated by the long, narrow vertical arrows, relaxation to the lowest electronically excited state is thought to occur as depicted by the short, narrow arrows. The broad arrows mark the pathways that the two molecules are thought to follow upon relaxation from the first electronically excited state.



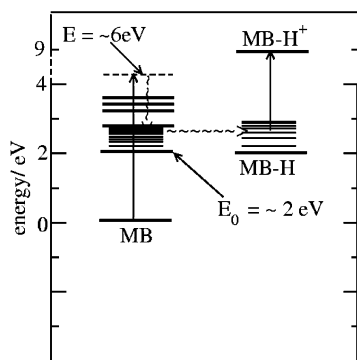


**Figure 7.** A Jablonski-type diagram illustrating the photoinduced dehydrogenation-photoinduced ionization process thought responsible for producing the dehydrogenated metal–DNA base (MB–H) cations observed in the mass spectra. Electronic states are shown as thick horizontal lines and the vibrational manifold associated with each state is shown as a group of thinner lines. The vertical lines depict the photoabsorption events while the squiggle depicts radiationless relaxation.  $E$  is the energy of the photon and  $E_0$  is the DFT-predicted energy required to dehydrogenate the neutral metal–base (MB) adduct. The energetics shown are derived from the DFT and experimental results as described in the text.

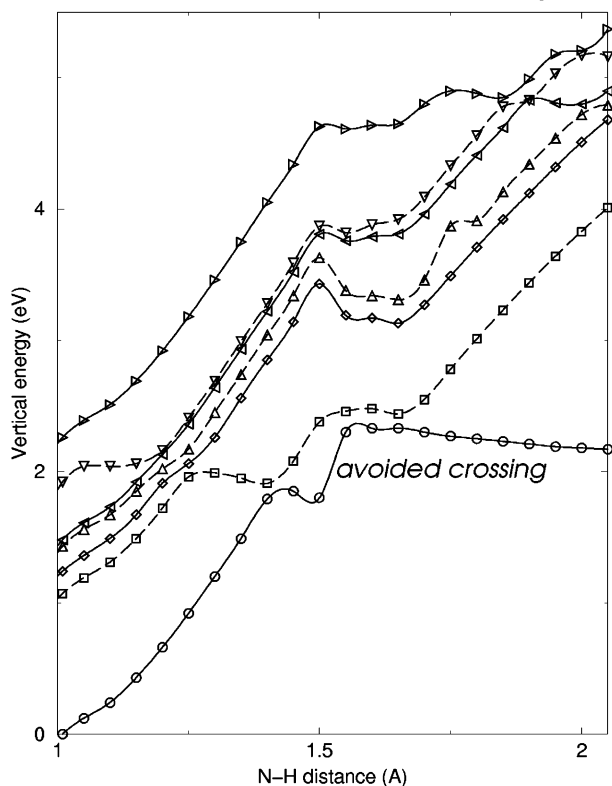


**Figure 8.** Theoretical potential energy curves of the electronic states of Al–guanine as a function of the N–H bond length, where N is the five-membered ring-constituent nitrogen. An avoided crossing between the ground and first excited electronic states is labeled.

absorption of a second photon that ionizes the dehydrogenated species. In this context, the threshold energies measured (Table 1) correspond to the energy required to photoionize the nascent, vibrationally excited, dehydrogenated species. DFT indicates that 7 eV are required to ionize dehydrogenated metal–base complexes in their rovibronic ground states. Alternate mechanisms for the dehydrogenation, such as those involving participation of higher-energy dissociative states of the neutral or cation, cannot be precluded using these calculations but a qualitative picture of the effect of metals on neutral cytosine dehydrogenation at the energies considered can be drawn.

As seen in Figure 6, for both cytosine and Al–cytosine the DFT predicts a relatively high density of electronic states separated from the ground state by a significant energy gap. The high density of states predicted suggests many pathways for curve-crossing events and is consistent with the efficient nonradiative relaxation characteristic of the DNA bases.<sup>8,9</sup> The predicted gap between the ground and first electronically excited states is expected to function as a bottleneck for nonradiative relaxation to the ground state, in accord with the energy gap rule.<sup>11</sup> From these results, one expects that photoexcitation of cytosine or Al–cytosine to some of the higher energy states shown will be followed by efficient nonradiative relaxation (curve-crossing) events. Curve crossing from the first excited state to the ground state will be inefficient at near-equilibrium N–H bond lengths due to the relatively large energy gap between the two states. At longer N–H bond lengths, however, the potential energy curves associated with the two states approach each other and the gap is decreased, as seen in Figure 6. For cytosine the first excited-state potential energy curve approaches the ground-state potential almost tangentially at relatively long N–H bond distances. The tangential approach is expected to facilitate curve crossing to the ground state and manifest efficient nonradiative, nondissociative relaxation to this state.<sup>21</sup> This process is depicted by the arrows drawn in Figure 6. For Al–cytosine the curves associated with the first electronically excited state and the ground-state approach at a much more acute angle than is the case for cytosine, and curve crossing between them is therefore expected to be a much less favorable process. Accordingly, dissociation of the N–H along the first excited-state potential energy curve is expected to be much more probable, as depicted by the arrows shown in Figure 6. On the basis of the qualitative differences in the nature of the potentials shown in Figure 6, one can conclude from the DFT that post-photoexcitation dehydrogenation of Al–cytosine is likely to occur more readily than for cytosine. This conclusion is consistent with experiment where dehydrogenation of Al–cytosine is observed but no dehydrogenation of cytosine is evident. The theory therefore supports the notion that the photoinduced dehydrogenation observed is a nonstatistical process occurring via population of a repulsive electronic state.

To explore the generality of the nonradiative relaxation processes depicted in Figure 6 as a mechanism of dehydrogenation of metal–DNA base complexes, the electronic states of Al–guanine were also examined with DFT calculations using the same method described above for the Al–cytosine and cytosine systems. For Al–guanine, N–H dissociation of both the five-membered ring constituent N and the six-membered ring constituent N were examined. Dissociation of the five-membered ring N–H was found to be much more favorable, both energetically and in the context of the avoided curve-crossing mechanism described above for Al–cytosine. The results are shown in Figure 8.

As was the case for Al–cytosine, Al is predicted to have a significant effect on the nature of the electronically excited states of guanine and manifests an avoided curve-crossing between the ground and first electronically excited states not observed for guanine itself (data not shown). The result is similar to the Al–cytosine result and suggests that photoinduced dehydrogenation of Al–guanine is more probable than photoinduced dehydrogenation of guanine. The similarity of the results for Al–cytosine and Al–guanine suggests that the mechanism may be general and that complexation of guanine or cytosine with metals significantly increases the probability of dehydrogenation.

**Multiphoton-Excitation and Non-radiative Relaxation Processes in Metal–DNA Base Complexes.** For the metal–DNA base complexes, dehydrogenation is observed to occur over such a range of energies that it must often be the case that the initial photoexcitation is to a state other than the dissociative state responsible for dehydrogenation. Dehydrogenation of Al–guanine, for example, is observed at many different wavelengths between 157 and 210 nm as seen in Figure 3. For Al–cytosine, dehydrogenation is also observed to occur over a wide range of wavelengths.<sup>1</sup> The fact that significant amounts of dehydrogenated metal–base complexes are observed at many wavelengths, above the threshold energy, indicates that nonradiative relaxation from the initially excited states to the dissociative state are efficient consistent with the high density of states, as seen in Figure 6. Efficient nonradiative relaxation to lower energy electronic states is consistent with solution-phase data where lifetimes of excited states of the DNA bases can be less than a few picoseconds.<sup>5,10</sup> Similarly, nonradiative relaxation of excited states populated via 263 nm excitation of solution-phase DNA nucleosides is known to occur on the 290 to 540 ( $\pm 40$ ) fs range and is very efficient.<sup>8,9</sup> By analogy, our observation of dehydrogenation at many photoexcitation energies, between threshold and 7.9 eV (our highest energy laser), suggests that radiationless relaxation is efficient for many of the electronic states in gas-phase metal–DNA base complexes as well.

In Figure 4, plots of the log of signal intensity for guanine, Al–cytosine, and Al–guanine are shown as functions of the log of ionization laser fluence, for ionization at 218.55 nm. In accord with eq 4, the plots are found to be linear. For guanine, which has an ionization energy of 8.24 eV,<sup>22</sup> only two-photon processes can contribute to the signal intensity as 218.55 nm (5.6727 eV) laser light has insufficient energy to ionize the molecule. These processes can be either simultaneous absorption of two photons or initial population of a resonant state and subsequent ionization from this state. Slopes of plots such as those shown in Figure 4 are expected to be two or one for the two different processes, respectively. The deviation of the slope ( $1.6 \pm 0.2$ ) from the expected values is indicative of the occurrence of fragmentation.<sup>23</sup> This observation is consistent with post-ionization, photoinduced fragmentation competing with the molecular ionization process or indicative of competition between photodissociation via a simultaneous two-photon absorption and nondissociative ionization via sequential absorption of two photons (resonant-enhanced ionization). Post-ionization fragmentation of guanine has been observed at lower photoexcitation energies.<sup>13</sup> As the ionization laser power used in our experiments was relatively small (less than 100  $\mu\text{J}$  pulse<sup>-1</sup> and not focused), any multiphoton processes occurring must be efficient. Other ionization wavelengths examined include 207.00, 212.50, and 222.50 nm. At 207.00, 212.50, and 218.55 nm, two-photon processes made the dominant contribution to the mass spectral peaks associated with Al<sub>n</sub>–guanine<sub>m</sub> species. At 222.50 nm, single-photon processes were dominant. As the probability of single- or multiphoton processes depends on the availability and lifetime of electronically excited states, such a dependence on wavelength is expected. In general, the dominance of multiphoton contributions to the mass spectral intensities at the relatively low laser fluences employed in these experiments is remarkable.

A possible reason for the dominance of two-photon processes in the power-dependence data is that the two-photon ionization process is a resonantly enhanced process involving population of an intermediate electronically excited state with a short

lifetime. In accord with eq 4, for resonantly enhanced two-photon ionization, log plots like those shown in Figure 4 will have slopes near two only if  $\gamma$ , the rate of nonradiative relaxation from the intermediate state, is large. That is, when rapid radiationless relaxation from the resonant state, A\* in eqs 1–3, occurs. For gas-phase DNA bases, the possibility of such rapid nonradiative relaxation has been reported: the occurrence of efficient intersystem crossing from electronically excited states has been postulated for gas-phase guanine.<sup>13</sup> In solution phase, nonradiative relaxation occurs on the picosecond or less time scale.<sup>8,9</sup> Rapid nonradiative relaxation is also consistent with the dehydrogenation mechanism proposed above. In light of this evidence, attributing the dominance of two-photon processes, in the power-dependence data, to resonant enhancement is reasonable.

## Summary and Conclusions

In circumspect, the results presented all indicate that the photochemistry and photophysics of gas-phase, metal–DNA base complexes are dominated by relatively rapid and efficient nonradiative relaxations from electronically excited states. For photoinduced dehydrogenation, which is observed for Mn–guanine, Al–cytosine, Al–guanine, and Al–guanine–cytosine, our results indicate that nonradiative relaxation to an electronic state repulsive in the N–H coordinate occurs. Dehydrogenation occurs upon excitation of the metal–base complexes at many different wavelengths, suggesting that relaxation to the repulsive state occurs efficiently regardless of the electronic state initially excited. Efficient, relatively rapid nonradiative relaxation processes are also thought to impact on multiphoton, resonant-excitation processes which have dependencies on laser fluence characteristic of nonresonant processes due to the short-lived nature of the electronic states excited initially. Multiphoton absorption processes are found to make the dominant contribution to the mass-spectral signal intensity at most of the wavelengths examined. We propose that these are resonantly enhanced processes and therefore highly probable but that the intermediate states populated are short-lived, consistent with the observed nonresonant-type dependence of the mass spectral signal intensity on laser fluence.

## References and Notes

- Pedersen, D. B.; Zgierski, M. Z.; Denommee, S.; Simard, B. *J. Am. Chem. Soc.* **2002**, *124*, 6686.
- Sponer, J.; Spöner, J. E.; Gorb, L.; Leszczynski, J.; Lippert, B. *J. Phys. Chem. A* **1999**, *103*, 11406.
- Lahav, M.; Heleg-Shabtai, V.; Wasserman, J.; Katz, E.; Willner, I.; Durr, H.; Hu, Y.; Bossmann, S. H. *J. Am. Chem. Soc.* **2000**, *122*, 11480.
- Mirkin, C. A.; Letsinger, R. L.; Mucic, R. C.; Storhoff, J. J. *Nature* **1996**, *382*, 607.
- Daniels, M.; Hauswirth, W. *Science* **1971**, *171*, 675.
- Vinogradov, I. P.; Zemskikh, V. V.; Dononova, N. Y. *Opt. Spectrosc.* **1974**, *36*, 344.
- Daniels, M. *Photochemistry and Photobiology of Nucleic Acids*, Vol. 1; Academic Press: New York, 1976.
- Pecourt, J. L.; Peon, J.; Kohler, B. *J. Am. Chem. Soc.* **2000**, *122*, 9348.
- Pecourt, J. L.; Peon, J.; Kohler, B. *J. Am. Chem. Soc.* **2001**, *123*, 10370.
- Reuther, A.; Iglev, H.; Laenen, R.; Laubereau, A. *Chem. Phys. Lett.* **2000**, *325*, 360.
- Avouris, P.; Gelbart, W. M.; El-Sayed, M. A. *Chem. Rev.* **1977**, *77*, 793.
- Duncan, M. A.; Dietz, T. G.; Liverman, M. G.; Smalley, R. E. *J. Phys. Chem.* **1981**, *85*, 7.
- Nir, E.; Grace, L.; Brauer, B.; de Vries, M. S. *J. Am. Chem. Soc.* **1999**, *121*, 4896.
- Parker, D. H.; Berg, J. O.; El-Sayed, M. A. In *Advances in laser chemistry*; Zewail, A. H., Ed.; Springer-Verlag: Berlin, 1978.

- (15) Stemp, E. D. A.; Holmlin, R. E.; Barton, J. K. *Inorg. Chim. Acta* **2000**, 297, 88.
- (16) Burda, J. V.; Sponer, J.; Hobza, P. *J. Phys. Chem.* **1996**, 100, 7250.
- (17) Burda, J. V.; Sponer, J.; Leszczynski, J.; Hobza, P. *J. Phys. Chem. B* **1997**, 101, 9670.
- (18) Sponer, J.; Burda, J. V.; Sabat, M.; Leszczynski, J.; Hobza, P. *J. Phys. Chem. A* **1998**, 102, 5951.
- (19) Jakubek, Z. J.; Simard, B. *J. Chem. Phys.* **2000**, 112, 1733.
- (20) Pedersen, D. B.; Simard, B.; Moussatova, A.; Martinez, A. *J. Phys. Chem. A.*, submitted.
- (21) Sobolewski, A. L.; Domcke, W. *Chem. Phys.* **2000**, 259, 181.
- (22) Hush, N. S.; Cheung, A. S. *Chem. Phys. Lett.* **1975**, 34, 11.
- (23) Fisanick, G. L.; Eichelberger, T. S.; Heath, B. A.; Robin, M. B. *J. Chem. Phys.* **1980**, 72, 5571.